

General Disclaimer

One or more of the Following Statements may affect this Document

- This document has been reproduced from the best copy furnished by the organizational source. It is being released in the interest of making available as much information as possible.
- This document may contain data, which exceeds the sheet parameters. It was furnished in this condition by the organizational source and is the best copy available.
- This document may contain tone-on-tone or color graphs, charts and/or pictures, which have been reproduced in black and white.
- This document is paginated as submitted by the original source.
- Portions of this document are not fully legible due to the historical nature of some of the material. However, it is the best reproduction available from the original submission.

(NASA-TM-79223) FATIGUE BEHAVIOR OF SiC
REINFORCED TITANIUM COMPOSITES (NASA) 19 p
HC A02/MF A01 CSCI 11D

N79-30296

Unclas
31861

G3/24

NASA Technical Memorandum 79223

FATIGUE BEHAVIOR OF SiC REINFORCED
TITANIUM COMPOSITES

R. T. Bhatt and H. H. Grimes
Lewis Research Center
Cleveland, Ohio



Prepared for the
Symposium on Fatigue of Fibrous Composite Materials
sponsored by the American Society for Testing and Materials
San Francisco, California, May 22-23, 1979

FATIGUE BEHAVIOR OF SiC REINFORCED TITANIUM COMPOSITES

by R. T. Bhatt and H. H. Grimes

National Aeronautics and Space Administration
Lewis Research Center
Cleveland, Ohio 44135

Abstract

The low cycle axial fatigue properties of 25 and 44 fiber volume percent SiC/Ti(6Al-4V) composites were measured at room temperature and at 650° C. At room temperature, the S-N curves for the composites showed no anticipated improvement over bulk matrix behavior. Although axial and transverse tensile strength results suggest a degradation in SiC fiber strength during composite fabrication, it appears that the poor fatigue life of the composites was caused by a reduced fatigue resistance of the reinforced Ti(6Al-4V) matrix. Microstructural studies indicate that the reduced matrix behavior was due, in part, to the presence of flawed and fractured fibers created near the specimen surfaces by preparation techniques. Another possible contributing factor is the large residual tensile stresses that can exist in fiber-reinforced matrices. These effects as well as the effects of fatigue testing at high temperature are discussed.

Introduction

Fiber reinforcement of a metal can often yield a composite with mechanical fatigue properties superior to those of the unreinforced metal. The predominant mechanism for this improvement is the fact that at the same fatigue stress level the cyclic stress on the reinforced matrix is reduced which correspondingly reduces the initiation and propagation of matrix fatigue cracks. Abundant examples of composite fatigue superiority over unreinforced metal are available in the literature. In many cases, however, the improvement is not attributed to matrix stress reduction but to other factors such as the deflecting and impeding role of the fibers and interfaces on the fatigue crack (1). Although these factors, as well as fiber flaws, reaction zones, residual stresses, etc. may have large effects on fatigue properties, their significance is often difficult to evaluate due to the overwhelming effect of matrix stress reduction. Thus, the importance of these other factors can only be evaluated in experiments where stress reduction effects are accounted for by comparing the composite matrix and the unreinforced metal fatigue properties at the same matrix stress.

The purpose of this experimental study is to evaluate on a microstructural level those factors which control the fatigue resistance of Ti(6Al-4V) metal reinforced with SiC fiber. This composite system was selected for study for several reasons. First, the titanium alloy matrix is considerably harder and more fatigue-failure prone than most of the composite metal-matrices previously studied. Second, the fatigue properties of the unreinforced matrix have been studied extensively (2). Based on these studies, it is anticipated that factors influencing matrix fatigue behavior such as notch sensitivity and residual stresses will be significantly modified in the composite to warrant investigation. Third, because both the fiber and the matrix in SiC/Ti(6Al-4V) composites deform elastically up to fracture of the composite at room temperature, it should be possible to estimate the matrix stresses during the fatigue test from elastic theory. With this information, then, one can eliminate the stress reduction factor from the composite fatigue data and thus better evaluate the influence of other microstructural factors on matrix behavior. Finally, no prior fatigue study of this composite system was found despite its potential for aerospace application.

Experimental

Materials: The SiC/Ti composite used in this study was manufactured by TRW using AVCO 142 μm (5.6 mil) SiC on carbon fiber and Ti(6Al-4V) alloy matrix. Unidirectional composite panels containing 14 or 18 plies sandwiched by 0.76 mm thick Ti(6Al-4V) cover skins were consolidated by foil/filament diffusion bonding methods described by Brentnall and Toth (3). The panels were pressed at 0.10 GN/m^2 (15,000 psi) for 30 minutes at a temperature of 870°C . Two volume fractions of fibers were used, 25 volume percent and 44 volume percent.

For reasons relating to faulty tooling dies used during diffusion bonding, the original material produced in this way was found to be less than fully dense, with some void areas appearing between the fibers in the plane of the lamina. Therefore, an additional hot isostatic pressing (HIP) was used to further consolidate the plates to the point where no voids were observable. In this "HIPing" process, the temperature was held at 843°C , below that used for diffusion bonding (870°C), and the time was limited to one-half hour. Subsequent microstructural examination of the fiber/matrix interface reaction zone revealed no voids and no significant increase of the

zone thickness. This interface zone, shown in Figure 1, was 0.5 μm thick, typical of well bonded SiC/Ti(6Al-4V) composites (3).

Fatigue and tensile specimens were cut from the plates to the dimensions shown in Figure 2. Both axial (0°) and transverse (90°) tensile specimens were prepared.

Testing procedures: Fatigue testing, both at room temperature and at elevated temperature, was done in a tension-tension mode, using an axial fatigue test facility developed at the NASA-Lewis Research Center. This facility which is described elsewhere (4) could be operated by a servo-controlled closed loop hydraulic system in either a load- or strain-controlled mode. All fatigue testing was conducted at 0.5 Hz in a load-controlled mode. Conventional wedge-type grips were found to be unsuitable for these tests due to slipping within the grips. To overcome this problem, a new grip assembly was designed and is shown schematically in Figure 3.

In the elevated temperature fatigue tests, the specimens were resistance heated with chopped AC currents of 600 amperes. The grips were water cooled to prevent any creep or relaxation of the gripping during high temperature tests. The temperature at the center of the specimen was monitored by an attached chromel-alumel thermocouple and held constant within $\pm 1^\circ\text{C}$.

Tensile testing at room temperature was accomplished in a standard Instron machine using conventional wedge-type grips and a constant cross-head speed of 0.51 mm/sec (0.02 in./min). Room temperature elastic modulus and Poisson's ratio measurements were made on the composite using the fatigue testing facility. The axial strain was measured with two resistance-type strain gauges cemented on parallel sides of the specimen. The diametrical strain was measured using a diametrical extensometer clamped onto the specimen. Load was changed in increments of 200 pounds to trace the load-strain plots.

Measurement was made of the tensile strength of SiC fibers both before consolidation into a composite and after removal from the composite by acid dissolution of the matrix using a hot 50 percent HCl-50 percent H_2O solution. Fibers of each type were pulled to failure in an Instron testing machine using the test method described in Reference 5.

Results and Discussion

Tensile data: The room temperature elastic modulus, Poisson's ratio, and tensile strength as a function of volume percent fiber are shown in Fig-

ures 4 to 6 for the SiC/Ti(6Al-4V) composites used in this study. The data points indicate the range and average value for each volume fraction. Typically, eight tests were performed for each data point. Also included for comparison purposes are the averaged data of Brentnall and Toth (3) and Tsareff, et al. (6). Our measured values of axial modulus, E_{11} , and Poisson's ratio, ν_{12} , were found to agree well with the calculated "rule-of-mixtures" values based on the data for pure Ti(6Al-4V) (2) and for SiC fibers (7). The axial tensile strengths, however, while consistent with the data of Reference 3, show rather low values compared with the rule-of-mixtures predictions based on an average tensile strength of the as-received fiber of 3.4 GN/m^2 (500,000 psi) and a value of 0.85 GN/m^2 (124,000 psi) for the stress on the matrix strained to the fracture strain of the fiber (0.008). The average measured value of axial tensile strength was 1.03 GN/m^2 (150,000 psi) for the 44 volume percent composite and 0.86 GN/m^2 (125,000 psi) for the 25 volume percent composite. The corresponding calculated rule-of-mixtures values are 1.99 GN/m^2 (289,000 psi) for the 44 volume percent composite and 1.50 GN/m^2 (218,000 psi) for the 25 volume percent composites.

The transverse tensile strength for the 44 volume percent composite, 0.27 GN/m^2 (40,000 psi), was also found to be low when compared with the ultimate tensile strength we measured for an annealed Ti(6Al-4V) alloy, 0.92 GN/m^2 (135,000 psi). For no fiber/matrix bonding, a lower bound can be estimated for the transverse tensile strength σ_T from the Equation (4a) of Reference 8:

$$\sigma_T = \sigma_m \left[1 - 2 \left(\frac{V_f}{\pi} \right)^{1/2} \right]$$

where σ_m is the UTS of the matrix and V_f the volume fraction of the fiber. For $V_f = 0.44$, the σ_T value obtained is 0.23 GN/m^2 (34,000 psi). Since our measured value of transverse strength was slightly higher than the calculated value for no bonding, it may be concluded that the fibers are only partially bonded to the matrix, or that the interfacial bond is weak, or that the fiber's transverse strength was low.

To understand the mechanisms responsible for the low composite strength values, SEM micrographs were taken. Typical tensile fracture surfaces of specimens stressed in the axial and transverse directions are shown in Figures 7 and 8, respectively. The fracture surface of Figure 7 gives no evidence of extensive fiber pull-out, characteristic of poor bonding. This

favors the argument for fiber strength degradation rather than weak or partial interface bonding. The fracture surface of Figure 8 also supports this view in that fiber splitting occurs in preference to fiber debonding. As part of SiC fiber manufacturing, a thin carbon coating is deposited on the fiber surface to improve handleability by decreasing surface flaw sensitivity. Any process which mechanically or chemically degrades this coating will result in fiber weakening. This effect was discussed by DeBolt and Krukonis (7) as causing SiC fiber strength decreases of 0.69 to 1.38 GN/m² (100,000 to 200,000 psi).

To determine whether fiber degradation did occur, tensile tests were conducted on 2.54 cm gauge lengths of as-received SiC fibers and on fibers chemically removed from the 44 volume percent composite after consolidation. The average of the strengths measured for 65 fibers removed from the as-fabricated composite was 2.07 GN/m² (300,000 psi) compared with an average value of 3.45 GN/m² (500,000 psi) for 30 as-received SiC fibers. Thus while it is not completely understood what the degradation mechanism is, it appears that this coating may be rendered ineffective by composite fabrication with a titanium matrix. If we use our measured average value of 2.07 GN/m² (300,000 psi) for the degraded fiber strength in the rule-of-mixtures equation and the stress on the matrix for a strain equal to the fiber fracture strain (0.0045) we obtain an axial tensile strength of 1.20 GN/m² (175,000 psi) which is in better agreement with our measured value of 1.03 GN/m² (150,000 psi).

Fatigue Data

Axial low cycle fatigue testing of 25 and 44 volume percent SiC/Ti(6Al-4V) composites was done at room temperature and 650^o C at a stress ratio $R = 0.0$ ($R = \text{minimum stress}/\text{maximum stress}$). The data obtained are presented in Figure 9 as applied maximum external stress versus number of cycles to failure (S-N curves). Matrix fatigue behavior at room temperature for annealed Ti(6Al-4V) bar stock of identical specimen configuration is also shown in this figure for comparison. It can be seen that the room temperature S-N curves for 25 volume percent and 44 volume percent composites and the unreinforced matrix alloy are all quite similar up to 10⁶ cycles, the maximum number of cycles tested. No definite approach to a fatigue limit is indicated up to this cycle level for these composite materials, nor is any beneficial effect noted by the presence of fibers.

The S-N curves for composites fatigued at 650° C are also shown in Figure 9. The curves, while similar to the room temperature S-N curves, have shorter cycle lifetimes for the same maximum stress values. At both temperatures, little difference can be observed between the 25 volume percent and the 44 volume percent composites data.

In contrast to the fatigue data for many of the other metal-matrix composites studied (1), it appears that the SiC/Ti(6Al-4V) system does not exhibit the anticipated improvement in room temperature fatigue properties with fiber reinforcement. The reason for this and for the apparent lack of dependence on fiber loading was further investigated in this study.

Because there exists no indication that ceramic fibers such as SiC or boron are subject to fatigue damage (9), one can conclude that the lifetime-limiting processes in ceramic fiber reinforced metal matrix composites is the initiation and/or growth of the fatigue crack in the matrix. In the composite, the matrix carries only a fraction of the load experienced by the monolithic matrix material alone in a comparable test. Thus, any effects in the matrix due to weak interfaces, stress concentrations or flaws, tensile residual stresses, work hardening or softening, etc. on crack initiation or propagation may be overwhelmed by the fatigue life improvement due to the reduced strain on the matrix. For this reason, the room temperature fatigue strength data of Figure 9 were replotted in Figure 10 as matrix strain amplitude vs. cycles-to-failure in order to compare the matrix in the composite and the unreinforced matrix material under conditions of equal cyclic strain. This plot is possible for SiC/Ti(6Al-4V) for two reasons. First, at room temperature, the fatigue and fracture strains observed for this composite were all within the elastic limit of both the fiber and the matrix. The load-deflection curves were indeed linear. Second, it appears that the amplitude of the matrix cyclic strain remains constant throughout the load controlled fatigue test. For this to be so, the fatigue life of the matrix would have to be controlled almost entirely by fatigue crack initiation time rather than crack propagation time. Support for this can be found in the literature for this alloy (10) and for the composite in the results of the following experiment designed to determine the relative importance of matrix crack initiation and crack propagation on fatigue life.

Several fatigue specimens were instrumented within the gauge length with probes to measure the D.C. resistance throughout the room temperature fatigue test. The resistance during cycling remained constant to within ±1 percent

throughout over 90 percent of the test duration, after which it increased exponentially to the time of specimen failure. A visible fatigue crack was observed within a few thousand cycles after the resistance increase. The resistance and visual observation of the fatigue crack confirm a mechanism in which the greater part of the fatigue life is spent in crack initiation, followed by a rather rapid crack growth to failure.

In addition, metallography carried out on the fatigue fractured specimens shows very few secondary cracks, further supporting the idea that fatigue crack initiation time is longer than the propagation time.

Having thus established the validity of Figure 10, let us now examine its two primary implications. Clearly, at a constant cyclic strain, the composite fatigue lifetime is reduced from that for the unreinforced matrix, suggesting that incorporation of the SiC reinforcement serves to degrade the fatigue properties of Ti(6Al-4V). In addition, increasing the fiber content from 25 volume percent to 44 volume percent appears to further reduce the lifetime, but only slightly.

One possible factor for the reduced fatigue behavior of the titanium composite is the presence of flawed and fractured fibers in the surface region of the specimens which could serve as initiation sites for the fatigue crack. The role of such flaws in facilitating fatigue crack initiation has long been known (1). To establish the presence of the flawed and fractured fibers in the surface of the specimen and their role in fatigue failure, metallographic investigation was carried out on the as-received and fatigue-fractured specimens. Figure 11(a), a photomicrograph of the machined surface of the as-received composite, shows such fractured fibers. Removal of the first two layers of the fibers by careful grinding and polishing produced no evidence of the broken or abraded fibers in the interior of the specimen. Thus we conclude that the surface fiber cracks occurred during specimen machining. Photomicrographs of the fatigue-fractured specimens indicate that the matrix fatigue cracks always initiated from these broken surface fibers (Fig. 11(b)). Metallographic analysis of the entire cross section of the fatigued specimen failed to produce any clear evidence of fatigue crack initiation at internal sites or even at the unmachined specimen surface. Thus, although fiber reinforcement reduces the matrix strain and thereby increases fatigue life, the presence of fractured and flawed fibers can also shorten the matrix crack initiation time and thus shorten the fatigue life in SiC/Ti(6Al-4V).

Another possible factor contributing to the poor fatigue resistance of SiC/Ti(6Al-4V) composites compared to unreinforced Ti- (6Al-4V) is the internal state of stress in the composite. Cooling of composites from the fabrication temperature can introduce residual stresses into the composite because of the difference in thermal expansion coefficients of the fibers and the matrix. Even though quantitative estimates of the magnitude of these residual stresses are rather difficult due to possible plastic relaxation of the matrix at high temperatures, one can assume elastic matrix behavior during cooling from the fabrication temperature and thus calculate the maximum residual stress in the matrix, σ_R , from the equations used by Schaefer, et al. (11)

$$\sigma_R = \left[\frac{E_m (\alpha_m - \alpha_f) (T_c - T_o)}{\frac{E_m V_m}{E_f V_m} + 1} \right]$$

where T_c is the composite consolidation temperature, T_o room temperature, α thermal expansion coefficient, E elastic modulus, V fiber volume fraction, and subscripts m and f refer to matrix and fiber, respectively. Using $T_c = 870^\circ \text{C}$ and values for α_m , α_f , E_f , and E_m from Reference 12, the residual matrix stress, σ_R , was calculated for various volume fractions of fiber in the composite. The calculated values in Figure 12 show that the matrix could be under a tensile stress as large as 0.38 GN/m^2 (56,000 psi) for the 44 volume percent SiC/Ti-(6Al-4V) composite. Preliminary X-ray line broadening studies on our as-received composite do, in fact, indicate the presence of residual stresses, but to date we have not been able to quantify them sufficiently for comparison with the calculated values.

The presence of a tensile residual stress in the matrix can be an additional source of reduced fatigue behavior in the composite. For example, from Reference 2, we learn that increasing the mean stress, at a constant cyclic stress, decreases the fatigue life of Ti(6Al-4V). This is indicated in the Goodman diagram of Reference 2 replotted here in Figure 13. The fatigue behavior of the matrix in our composites can be compared with the fatigue data of Reference 2 for Ti(6Al-4V) assuming the calculated residual stresses of Figure 12 to be present. As indicated by the insert of Figure 13, the mean stress on the matrix in our composites is obtained by adding half of the component of the applied cyclic stress experienced by the matrix σ_s , to the calculated tensile residual stress $\sigma_r = \sigma_{\min}$ for the two fiber volume fractions

studied. The resulting alternating versus mean stresses calculated from the best fit data of Figure 10 are plotted as the solid lines in Figure 13 for 10^4 , 3×10^4 , and 10^5 cycle lives.

Several interesting conclusions result from the comparison of these plots with the Ti(6Al-4V) fatigue data of Reference 2. First, the fatigue behavior of the matrix in our composite is similar to that of Ti(6Al-4V) in a notched condition. Thus, not only do the fibers provide no beneficial effect except to reduce the matrix stress, it is likely that their presence provides additional notch sensitivity to the matrix material, reducing its fatigue properties. Second, cooldown of the composite from the fabrication temperature to room temperature can produce residual stresses in the matrix which further reduce the matrix fatigue behavior. This reduction is proportional to the fiber volume fraction and can account for the observed decrease of fatigue properties with increased fiber content. Examined together, however, it appears that the fiber notch effect has a much more significant degrading effect on matrix fatigue than the residual stress effect.

The understanding of the high temperature fatigue results is complicated by several changes in the composite due to the temperature. These include: (1) a marked decrease in the strength and an increase in the ductility of the matrix, (2) relief of any tensile residual stress in the matrix, (3) relief of any compressive residual stress in the fibers, (4) an increase in the fraction of the load carried by the fibers, (5) a possible increase in the interface reaction layer, and (6) a general reduction in the stress intensity factor at the tip of a matrix crack. Item (1) is known to decrease matrix fatigue resistance (Ref. 2). Items (2), (4), and (6) might be expected to increase matrix fatigue resistance, Item (3) might be expected to have no effect, and Item (5) could go either way. In addition, there is no fatigue data available in the literature for the matrix beyond 500°C . Our own efforts to run fatigue tests at 650°C were unsuccessful because of excessive creep of the specimens. Without this comparison, interpretation of the results in terms of the above factors becomes rather speculative and was not attempted in this study.

Summary and Conclusions

The strength and fatigue behavior of SiC/Ti(6Al-4V) composites can be summarized as follows:

1. While measured axial elastic moduli and Poisson's ratios appear to agree with the rule-of-mixtures values, the axial and transverse tensile

strengths are distinctly lower. This strength disparity can be resolved if the fiber strength used in the calculation is that measured for fibers removed from the composite after consolidation. The low fiber strengths thus measured probably result from the return of surface flaw sensitivity of the SiC fibers due to abrasion or surface reaction during fabrication.

2. The room temperature S-N curves for this composite system indicate no enhancement, in fact, even a reduction of fatigue life at a given stress amplitude when compared with unreinforced matrix fatigue life. The fact that the composite deforms elastically at room temperature coupled with the observation that fatigue crack initiation in the matrix accounts for the major portion of the fatigue life of this composite allows one to compare the room temperature fatigue data on the basis of matrix strain amplitude. Fractured and flawed fibers near the composite surfaces are found to be contributory to the reduction of matrix fatigue life through their effect on crack initiation time. Thermal residual stresses generated during composite fabrication are also considered to be a prime contributor to the degradation of matrix fatigue behavior and can explain the decrease in fatigue properties with increasing fiber content.

3. The explanation of the fatigue properties at high temperatures is complicated by unknown effects of matrix plasticity, modification of residual stresses, and interface reaction effects.

In summary, it appears that significant improvement in the fatigue properties of SiC fiber reinforced Ti(6Al-4V) may be achieved with the elimination of broken or abraded fibers and the elimination or reduction of possible residual tensile strains in the matrix. Both problems might be alleviated to some extent by the use of a softer matrix material. The increased plasticity should reduce stress concentrations at flaws and also relieve residual stresses.

References

1. Hancock, J. R., in "Composite Materials," First Ed., L. J. Broutman, Ed., Academic Press, New York, Vol. 5, Chap. 9, pp. 371-414.
2. Mayakuth, D. J., Monroe, R. E., Favor, R. J., and Moon, D., "Titanium Base Alloys/6Al-4V, DMIC Processes and Properties Handbook," Battelle Memorial Inst., Feb. 1971.
3. Brentnall, W. D. and Toth, I. J., "High Temperature Titanium Composites," Technical Report AFML-TR-73-223, Air Force Materials Lab., Dayton, Ohio, 1973.

4. Hirschburg, H. H., in "Manual on Low Cycle Fatigue Tests" ASTM STP 465, American Society for Testing and Materials, 1969, pp. 67-86.
5. Smith, R. J., "Changes in Boron Fiber Strength Due to Surface Removal by Chemical Etching," NASA-TN-T-5219, National Aeronautics and Space Administration, Wash., DC, 1976.
6. Tsareff, T. C., Sippel, G. R., and Herman, M., in "Metal-Matrix Composites," DMIC Memo 243, Defense Metals Information Center, Battelle Memorial Institute, May 1969.
7. DeBolt, H. and Krukonis, V., "Improvement of Manufacturing Methods for the Production of Low Cost Silicon Carbide Filament," Technical Report, AFML-TR-73-140, Air Force Materials Laboratory, Dayton, Ohio, 1973.
8. Cooper, G. A. and Kelly, A., in "Interfaces in Composites" ASTM, STP 452, American Society for Testing and Materials, 1969, p. 90.
9. Salkind, M. and Patarini, V., "Transactions," American Institute for Metallurgical Engineers, Vol. 239, p. 1268.
10. Weinburg, J. G. and Hanna, I. E., "An Evaluation of Fatigue Properties of Titanium and Titanium Alloys," TML Report No. 77, Titanium Metallurgical Laboratory, July 1957.
11. Schaefer, W. H. and Christian, J. L., "Evaluation of the Structure Behavior of Filament Reinforced Metal Matrix Composites," Technical Report, AFML-TR-69-36, Vol. 3, Air Force Materials Laboratory, Dayton, Ohio, 1969.
12. DiCarlo, J. A. and Maisel, J. E., "High Temperature Dynamic Modulus and Damping of Aluminum and Titanium Matrix Composites," NASA TN-79080, National Aeronautics and Space Administration, Washington, DC, 1979.

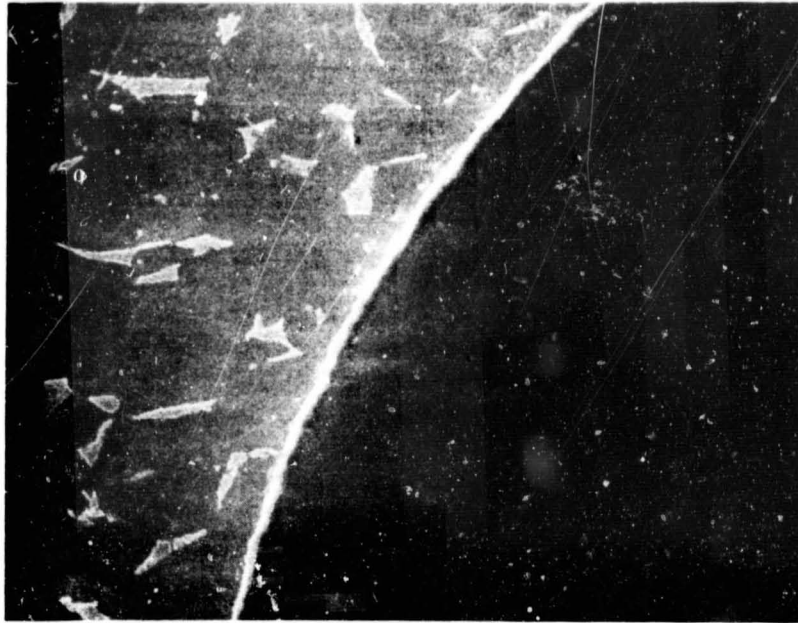


Figure 1. - Interface region of Ti-(6Al-4V)/SiC composite, in fabricated and hipped condition (3000x).

ORIGINAL PAGE IS
OF POOR QUALITY

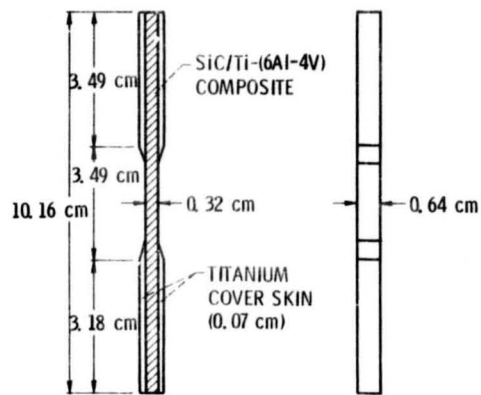


Figure 2. - Tensile and fatigue specimen geometry.

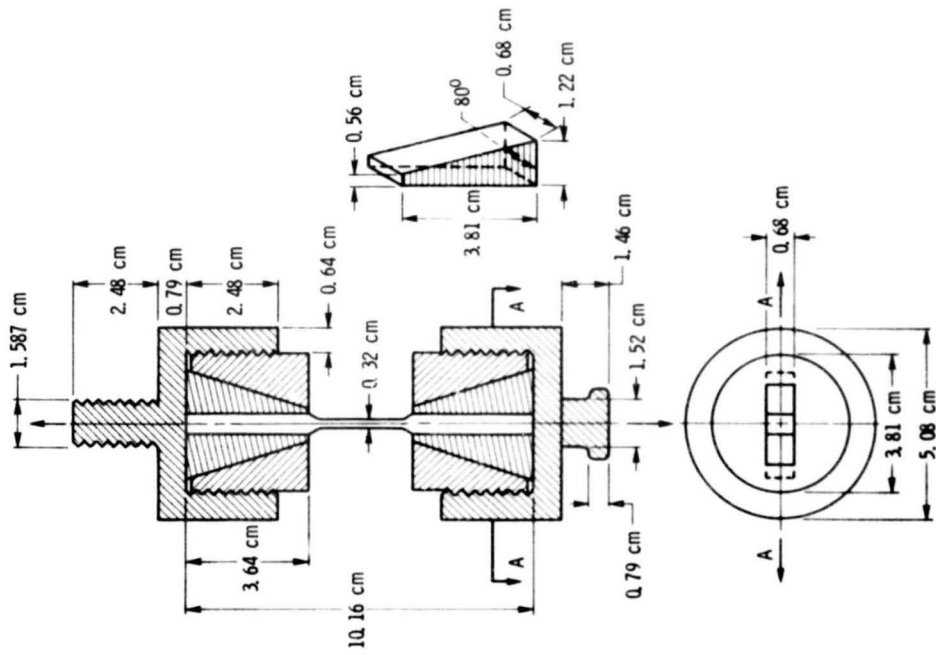


Figure 3. - Schematic diagram of the grip assembly.

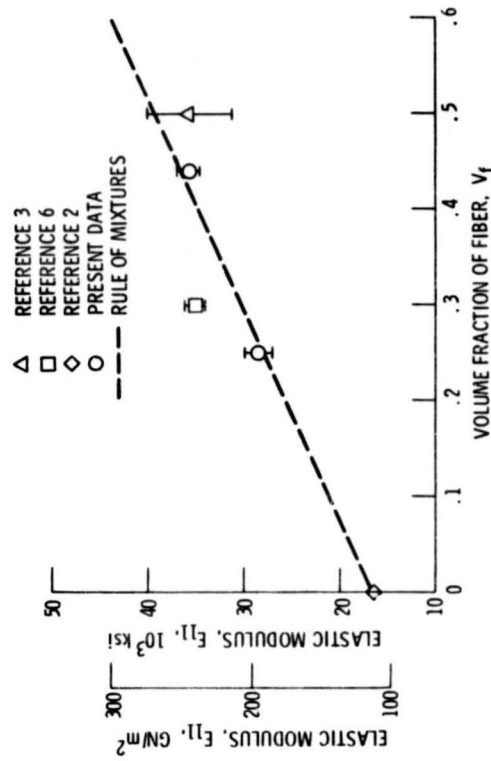


Figure 4. - Axial elastic modulus (E_{11}) of SiC/Ti-(6Al-4V) composite as a function of fiber content.

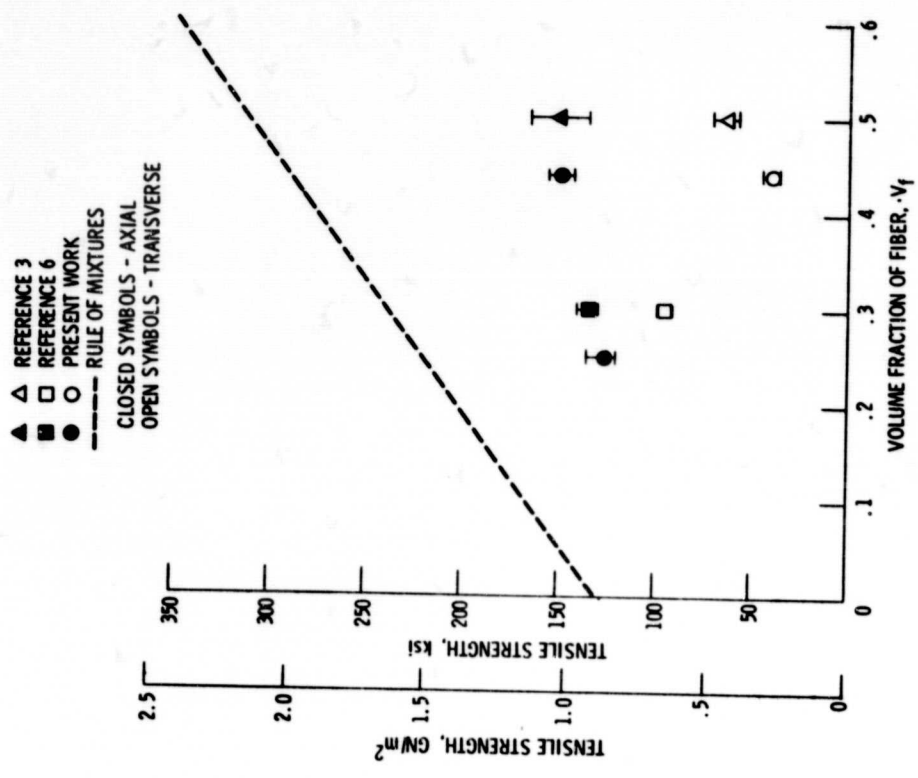


Figure 4. - Axial and transverse tensile strength of SiC/IT1-(6Al-4V) composite as a function of fiber content.

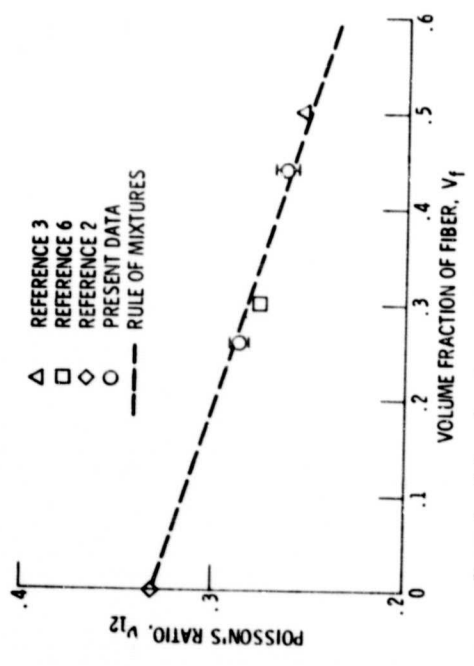


Figure 5. - Poisson's ratio (ν_{12}) of SiC/IT1-(6Al-4V) composite as a function of fiber content.

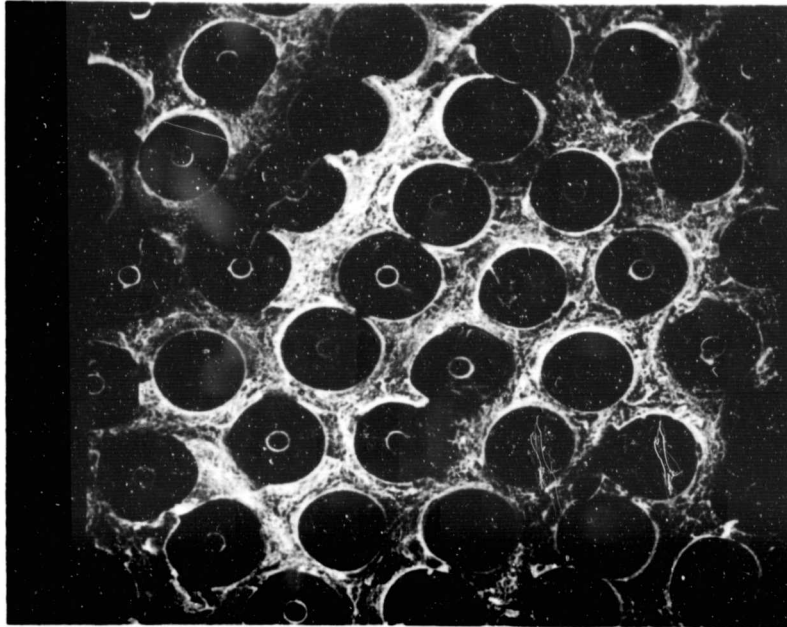


Figure 7. - Fracture surface of a SiC/Ti-(6Al-4V) composite stressed in axial direction (100x).

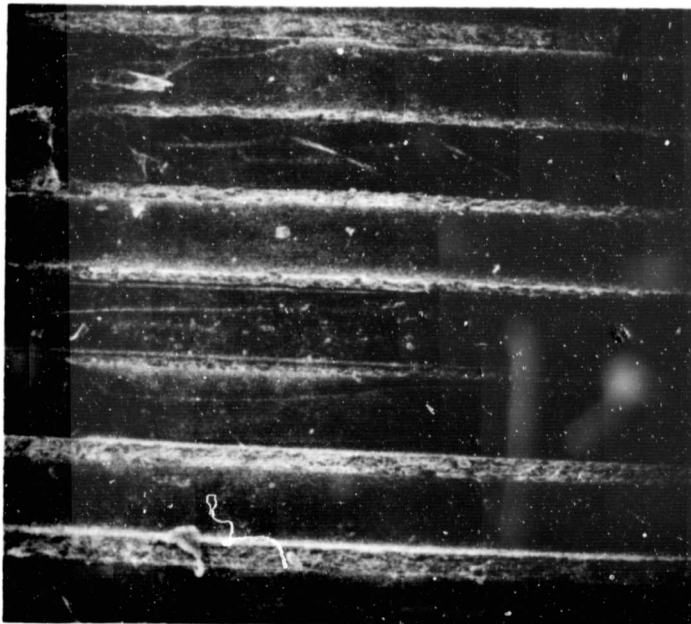


Figure 8. - Fracture surface of a SiC/Ti-(6Al-4V) composite stressed in transverse direction (100x).

ORIGINAL PAGE 15
OF 200

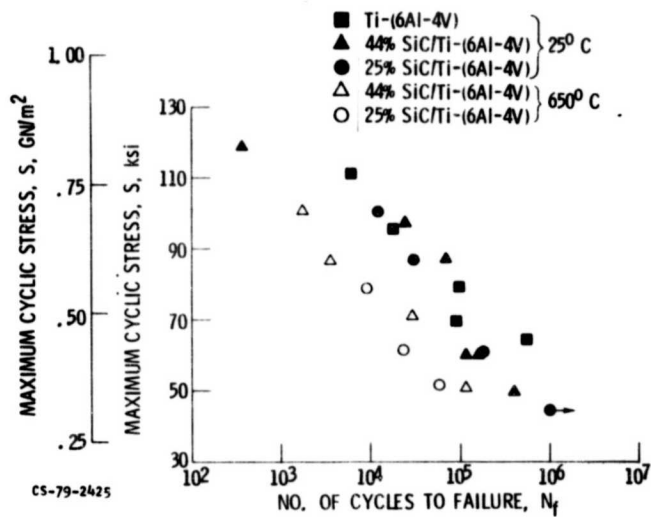


Figure 9. - Room and elevated temperature fatigue curves of SiC/Ti-(6Al-4V) system at a stress ratio of $R = 0.0$.

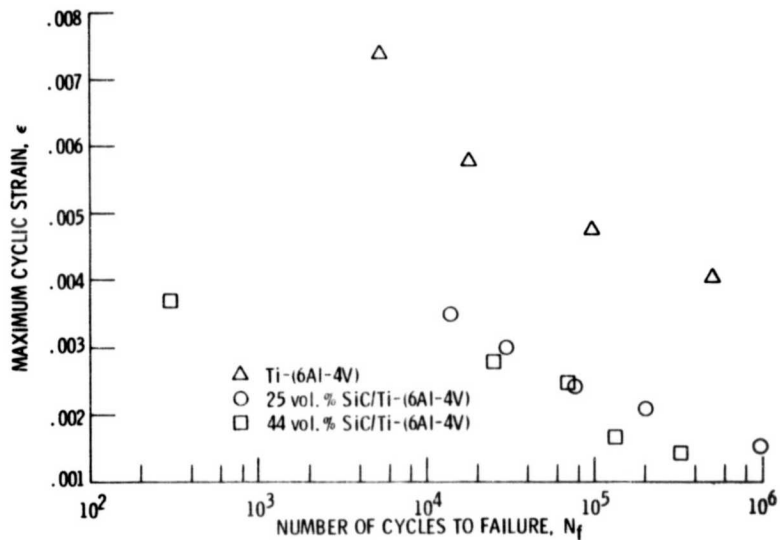
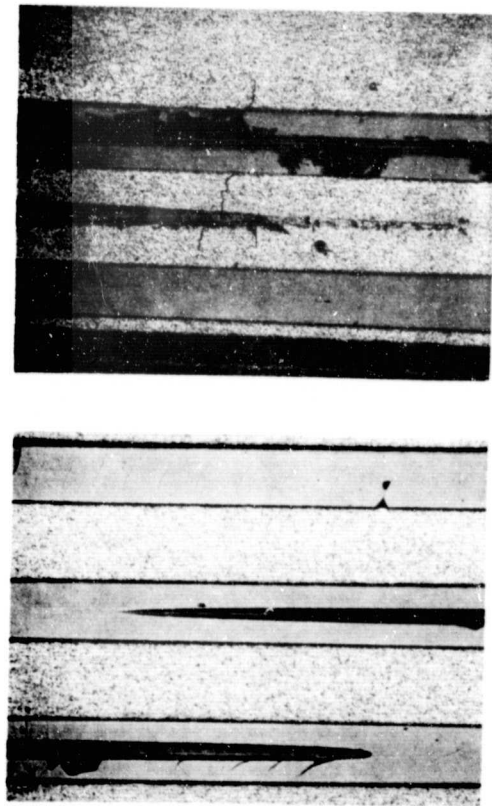


Figure 10. - Room temperature fatigue data of figure 9 for SiC/Ti-(6Al-4V) and Ti-(6Al-4V) plotted as the maximum matrix cyclic strain vs cycles to failure. The matrix strains in the composite are calculated using the composite moduli determined in this study.



(a) PHOTOMICROGRAPH OF A S-RECEIVED COMPOSITE SPECIMEN SHOWING THE CUT AND FRACTURED FIBERS ON THE MACHINED SURFACE, X100.

(b) PHOTOMICROGRAPH OF A FATIGUED SPECIMEN SHOWING FATIGUE CRACK INITIATION AT CRACKED SURFACE FIBER, X100.

Figure 11.

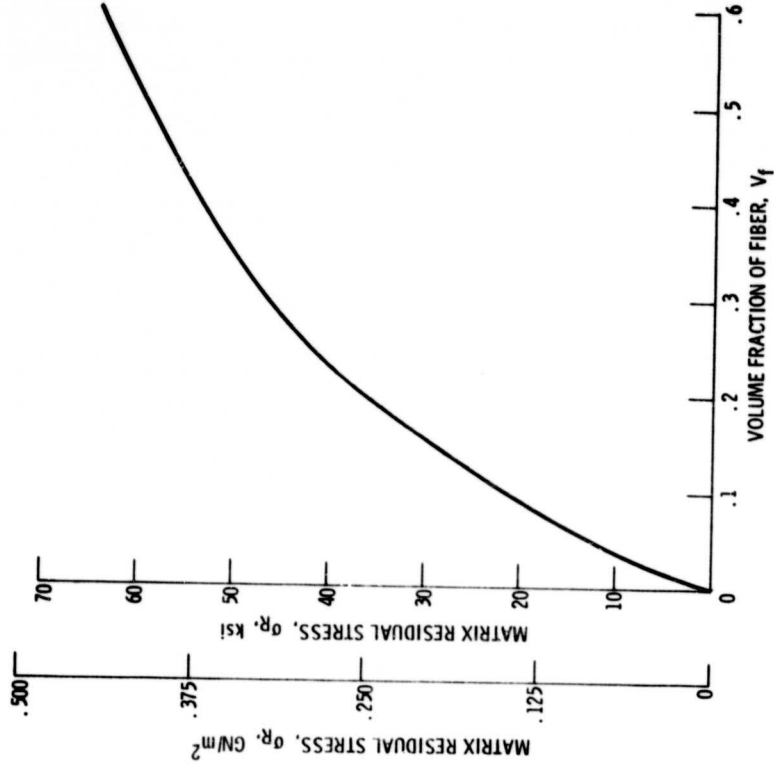


Figure 12. - Calculated matrix tensile residual stress, σ_R , in SiC/Ti-(6Al-4V) composite as a function of fiber content. Elastic matrix behavior is assumed during cooling from fabrication temperature of 870° C. Thermal expansion coefficients for the calculations obtained from reference 12.

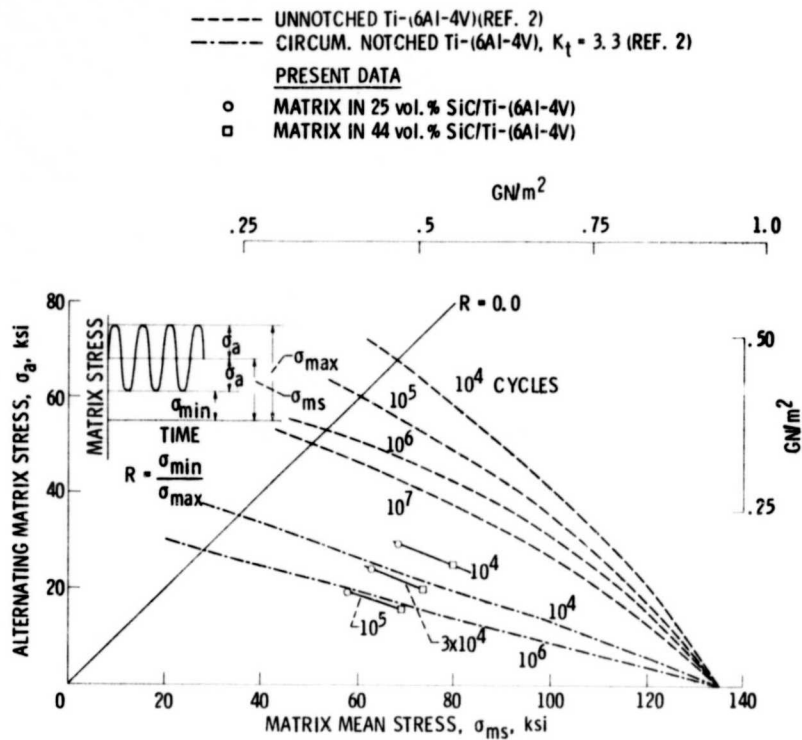


Figure 13. - Comparison of the Goodman diagram for notched and unnotched annealed Ti-(6Al-4V) with the properties of the Ti-(6Al-4V) matrix in the composites. The mean stress on the matrix in the composite was obtained by adding half of the component of the applied cyclic stress experienced by the matrix, σ_a , to the tensile residual stresses, σ_r , calculated for two volume fractions studied.